A Statistical Description of Arctic Level-Ice Pans, Using the USS *Gurnard* Ice-Draft Data Set

B.A. Hughes

Fisheries and Oceans Canada
Science Branch - Pacific Region
Institute of Ocean Sciences
P.O. Box 6000
Sidney, B.C. V8L 4B2

2003

Canadian Technical Report of
Hydrography and Ocean Sciences 229

Fisheries and Oceans Canada | Pêches et Océans Canada

Canada

Canadian Technical Report of Hydrography and Ocean Sciences

Technical reports contain scientific and technical information that contributes to existing knowledge but which is not normally appropriate for primary literature. The subject matter is related generally to programs and interests of the Ocean Science and Surveys (OSS) sector of the Department of Fisheries and Oceans.

Technical reports may be cited as full publications. The correct citation appears above the abstract of each report. Each report is abstracted in *Aquatic Sciences and Fisheries Abstracts* and indexed in the Department's annual index to scientific and technical publications.

Technical reports are produced regionally but are numbered nationally. Requests for individual reports will be filled by the issuing establishment listed on the front cover and title page. Out of stock reports will be supplied for a fee by commercial agents.

Regional and headquarters establishments of Ocean Science and Surveys ceased publication of their various report series as of December 1981. A complete listing of these publications is published in the *Canadian Journal of Fisheries and Aquatic Sciences*, Volume 39: Index to Publications 1982. The current series, which begins with report number 1, was initiated in January 1982.

Rapport technique canadien sur l'hydrographie et les sciences océaniques

Les rapports techniques contiennent des renseignements scientifiques et techniques qui constituent une contribution aux connaissances actuelles, mais qui ne sont pas normalement appropriés pour la publication dans un journal scientifique. Le sujet est généralement lié aux programmes et intérêts du service des Sciences et levés océaniques (SLO) du ministère des Pêches et des Océans.

Les rapports techniques peuvent être cités comme des publications complètes. Le titre exact paraît au-dessus du résumé de chaque rapport. Les rapports techniques sont résumés dans la revue *Résumés des sciences aquatiques et halieutiques*, et ils sont classés dans l'index annuel des publications scientifiques et techniques du Ministère.

Les rapports techniques sont produits à l'échelon régional, mais numérotés à l'échelon national. Les demandes de rapports seront satisfaites par l'établissement auteur dont le nom figure sur la couverture et la page du titre. Les rapports épuisés seront fournis contre rétribution par des agents commerciaux.

Les établissements des Sciences et levés océaniques dans les régions et à l'administration centrale ont cessé de publier leurs diverses séries de rapports en décembre 1981. Une liste complète de ces publications figure dans le volume 39, Index des publications 1982 du *Journal canadien des sciences halieutiques et aquatiques*. La série actuelle a commencé avec la publication du rapport numéro 1 en janvier 1982.

104-01403/

Canadian Technical Report of
Hydrography and Ocean Sciences 229

2003

A STATISTICAL DESCRIPTION OF ARCTIC LEVEL-ICE PANS, USING THE USS *Gurnard* ICE-DRAFT DATA SET

by

B.A. Hughes[1]

Fisheries and Oceans Canada
Science Branch - Pacific Region
Institute of Ocean Sciences
P.O. Box 6000
Sidney, BC V8L 4B2

[1]760 Walema Ave., Victoria BC V8Y 3B1
email: blythhughes@shaw.ca

© Her Majesty the Queen in Right of Canada, 2003
Cat. No. Fs 97-18/229E ISSN 0711-6764

Correct citation for this publication:

Hughes, B.A. 2003. A statistical description of arctic level-ice pans, using the USS *Gurnard* ice-draft data set. Can. Tech. Rep. Hydrogr. Ocean Sci. 229: vii + 35 p.

TABLE OF CONTENTS

TABLE OF CONTENTS iii
LIST OF TABLES iv
LIST OF FIGURES v
ABSTRACT vi
RÉSUMÉ vii
1. INTRODUCTION. 1
2. PANS AS "LEVEL" ICE 3
3. SPECTRA AND CORRELATION FUNCTIONS. 5
4. CONVOLUTION MODEL. 10
4.1 Pan Lengths 11
4.2 Standard Deviations 12
4.3 Means 17
4.4 Final Pdf 20
5. ESTIMATED DRAFT PROBABILITY DENSITY WITH THE NOISE REMOVED. 21
5.1 Approximate method 22
5.2 Wiener Filter 22
6. SLOPE DISTRIBUTION FUNCTION 24
7. DISCUSSION AND CONCLUSIONS 28
8. REFERENCES. 31
APPENDIX Standard Deviation Variability Test Analysis 33

LIST OF TABLES

Table 1. Ice Nomenclature 3
Table 2. Ranges of the Means, and Number of Pans in each Range 5
Table 3. Spectral Parameters 9
Table 4. Parameters for Probability Density of Pan Length 12
Table 5. Number of Independent Points 13
Table 6. Standard Deviation Values 17
Table 7. Gaussian Parameters for the Means 20
Table 8. Pdf Parameters for all the Populations 21
Table 9. Lognormal Parameters—Approximate Method for Noise Removal 23
Table 10. Lognormal Parameters—Wiener Filter Method 23
Table 11. Parameters for Computing the Slope Pdf's 26
Table 12. Correlation Values for Slope Pdf's 27

LIST OF FIGURES

Figure 1. Examples of selected pans 4
Figure 2. Probability density function for the level-ice drafts 6
Figure 3. Spectra of level-ice segments 7
Figure 4. Ice population 4 & 5 draft spectra 8
Figure 5. Probability density of ln(n) 11
Figure 6. Standard deviation (s) as a function of pan length (n) 15
Figure 7. Ice population 2 comparisons 16
Figure 8. Mean-values (M) as a function of pan length (n) 18
Figure 9. Distribution of the pan means (M) 19
Figure 10. $S(\kappa)$ as used in the Wiener filter 24
Figure 11. Theoretical and measured slope probability densities 27

ABSTRACT

Hughes, B.A. 2003. A statistical description of arctic level-ice pans, using the USS *Gurnard* ice-draft data set. Can. Tech. Rep. Hydrogr. Ocean Sci. 229: vii + 35 p.

Using the ice draft data measured from the USS *Gurnard* in the Beaufort Sea in 1976, an examination of the statistics of level-ice segments is given. It is shown that the standard deviations of the draft values within the segments are approximately constant for each ice draft population subset except for sampling variations, and that the mean draft values of the segments within each ice population are distributed as Gaussians. The length distributions of the segments are described tentatively as lognormals. Wavenumber spectra for the ice within the level-ice segments are given and it is shown that the high frequency measurement noise for this data set referred to by other researchers masks the spectra considerably. Parameters for the full draft probability density function with this noise removed by an approximate method, and also by a Wiener filter, are provided. With the noise removed the standard deviation of the ice using lognormal statistics is smaller and much more uniform across the different ice populations that are used to describe the ice field. A theoretical slope probability density curve is given based on lognormal statistics for the drafts including the deformed ice, and it is shown that it corresponds reasonably well to the measured values. The use of traditional "level" ice is also shown to be supported as a way of separating the thinner ice populations from the rubble.

RÉSUMÉ

Hughes, B.A. 2003. A statistical description of arctic level-ice pans, using the USS *Gurnard* ice-draft data set. Can. Tech. Rep. Hydrogr. Ocean Sci. 229: vii + 35 p.

On a analysé les statistiques sur les étendues de glace uniforme d'après les données sur le tirant d'eau de la glace recueillies en 1976 à bord du USS *Gurnard*, dans la mer de Beaufort. Il a été démontré que les écarts types des valeurs du tirant d'eau des étendues de glace ne varient presque pas d'une sous-population de valeurs à l'autre, à l'exception des variations dues à l'échantillonnage, et que les valeurs moyennes du tirant d'eau des étendues dans chaque population sont distribuées selon la loi normale de Gauss. On a déterminé provisoirement que la distribution des longueurs des étendues est logarithmonormale. En outre, on a déterminé les spectres du nombre d'onde pour la glace présente dans des étendues de glace uniforme et il est démontré que ces spectres sont considérablement voilés par le bruit de haute fréquence dans les mesures qui est associé à ce jeu de données et auquel d'autres chercheurs font référence. On a également déterminé les paramètres de la fonction de densité de probabilité du tirant d'eau total, lorsque ce bruit est éliminé par une méthode d'approximation et au moyen d'un filtre de Wiener. Une fois le bruit éliminé, l'écart type pour la glace établi d'après les statistiques logarithmonormales est moins grand et beaucoup plus uniforme pour les différentes populations utilisées pour décrire le champ de glace. D'après les statistiques logarithmonormales, on fournit une pente théorique de la courbe de densité de probabilité des tirants d'eau des radeaux, y compris pour la glace déformée, et on démontre que cette pente correspond raisonnablement bien aux valeurs mesurées. De plus, il est démontré qu'il est possible d'utiliser la glace « uniforme » classique pour distinguer les populations de glace plus mince de la blocaille.

1. INTRODUCTION

In April 1976, the American submarine USS *Gurnard* gathered a long track of ice draft data in the Beaufort Sea. The data were measured using an upward-looking sonar with a beam diameter of ~3 m, and data were taken approximately every 1.4 m along the track. The data have been subsequently interpolated to a uniform 1 m interval. The track comprised 3 nearly straight legs arranged approximately as ⊦ , and the total length was ~1400 km. Details are given in Wadhams and Horne (1980).

In a previous publication (Hughes 1991), the first 1,165 km of that ice draft data set were analyzed, and statistical measures were shown to be fitted quite well by a sequence of log-normals—7 were used in that publication—and they were each loosely identified with a part-icular ice type, i.e. young ice, thin ice, level ice…, in keeping with traditional ice typology. For numerical simulation purposes, a single standard deviation and a single mean were assumed to apply to each ice type population—each lognormal—and appropriate random deviates were used, and interspersed, to construct a simulated ice sheet.

In the present research the same 1,165 km data set is used (actually 1,165,044 data points with a basic 1-m spacing) and each ice type population is further considered to comprise a collection of ice segments each of which contains ice of that same population but which in total displays a possible range of standard deviations, means and lengths (or areas, as before). The purpose of the present paper is to examine the validity of this approach and to determine the statistical distributions associated with these ranges in order that they may be used in numerical simulations. To accomplish this each single lognormal, pertaining to each ice population, is allowed to be a convolution of a joint probability density function, convolved over standard deviation, mean and length (for the one-dimensional case) but all contained within that ice type population. This expresses it in its full generality, but it will be shown that the present data and analysis methods do not support retention of the full joint character of this inner pdf, instead, to the present accuracy of the analysis the three variables are essentially uncorrelated and so the joint probability density function becomes simply three independent univariate pdf's. Furthermore, the one defining standard deviation will be seen to be close to a δ-function and so it disappears completely. One of the basic conclusions coming out of the present research is that the pdf defining the means within each ice population is representable as Gaussians. It will be shown that this fits the *Gurnard* data set better than the earlier assumption of a single standard deviation *and* a single mean for each ice type population.

The present method of separating the data set into the basic ice segments—called "pans" in the following—consists of determining the "level" ice regions, identifying these as the desired pans, and apportioning them into the different ice draft populations in accordance with their

mean level ("young" ice and "thin" ice are lumped in with this same "level" ice criterion). The slope-based D1 technique of Wadhams and Horne (1980) has been used to determine the level ice, and although it is obvious from the data that this is a less-than-perfect method—because of the smearing effect of the filtering process across the ice segment edges it apportions only about 70% of the non-ridged (or non-background, non-deformed) ice—meaningful conclusions can still be obtained, even if they are not as precisely defined as they might be. It will be seen below that the level ice that is apportioned contains virtually all of the non-ridged ice (>93%) and very little of the deformed ice (<4%). Melling and Riedel (1995) have obtained good results using the Wadhams and Horne (1980) maximum-deviation D2 technique—and they prefer it over D1 because of its increased restrictiveness—thus D2 offers an attractive alternative to D1. A fractal approach has also been used with indications that fractal dimension may be a useful indication of level or non-level ice (Bishop and Chellis 1989) but with some partitioning limitations (Key and McLaren 1991).

For the distribution function of pan lengths (using the above "level" ice definition for pans), lognormal forms are fitted rather than the power-law forms given in the previous publication (Hughes 1991), and also obtained by Wadhams (1981) for a different set. The lognormals are considered to be more satisfactory than the power-laws not only because of their fit to the forms obtained from the data using the present analysis, but because of the power-law's preponderance of predicted segments with very short lengths, i.e. a few metres or less. However, no claim is being made for the theoretical appropriateness of the lognormal form, *per se*. The present analysis suggests a peak spanning the 100-metre region, and this is not too different from the results of Melling and Riedel (1996b) even though theirs is a cumulative estimate weighted by the length of the pan itself, and it is based on a different definition of "level."

The present work also underscores the presence of a low-level measurement noise field in the *Gurnard* data, previously reported by Wadhams and Horne (1980). Some further definitions and effects of this corrupting field are investigated, namely its wavenumber spectrum, its effect on the shallow draft pdf values, and its masking effect on the wavenumber spectrum of the ice draft in the pans. Attempts to "remove" it from the draft pdf by means of a deconvolving Wiener filter and an *ad hoc* approximate method are also described. In spite of the noise field, tentative wavenumber spectra are proposed and estimated for the pan drafts.

Finally the probability density of slopes is computed using the lognormal draft model (and some simplifying assumptions), and the fit to the measured slope histograms for the tested cases is provided and is considered to be quite satisfactory.

The nomenclature concerning ice types, and their definitions in terms of draft ranges, is not entirely satisfactory, so the present work is reported in terms of ice populations that are associated with the lognormal peaks as fitted and described previously (Hughes 1991). The over-

all rationale is that the ice field comprises several (more-or-less) distinct statistical populations each of which produces a peak in the draft pdf. The analysis deals with each population separately, and to make reference to these, each is simply given a numerical designation, with 1 referring to the population with the largest drafts and 5 to the population with the smallest. Table 1 gives the approximate draft range pertaining to each ice population (mean ± one sigma), as well as the lognormal peak number from Hughes (1991) and the Wadhams and Horne (1980) and McLaren (1989) nomenclatures. It should be noted that populations 2 and 3 will usually not be differentiated into 2a and 2b, or 3a and 3b, even though those are defined here.

Table 1. Ice Nomenclature

population	lognormal	draft range (m)	Wadhams & Horne	McLaren
5	7	<0.3—0.7	thin & some young	young and thin
4	6	0.7—1.08	young	medium
3b	5	1.5—1.9	young	thick, first year
3a	4	1.9—2.3	level	second year
2b	3	2.5—3.1	level	second year
2a	2	2.3—3.9	level	second and multiyear
1	1	2.9— >7.7	level & ridged	multiyear & deformed

2. PANS AS "LEVEL" ICE

The full *Gurnard* data set has been separated into approximate ice pan sets by producing slope data (by FFT) from the draft data, locally smoothing them over a horizontal span of 20 metres, and collecting the (draft) data segments whose points all have $|\text{slope}|_{20} \leq 0.025$. The FFT's were performed on contiguous 1024-long samples and these transforms were multiplied by the wavenumber k (and $\sqrt{-1}$) and by a Gaussian smoothing factor (equivalent to a 20 m box-car smoothing window) and were inverse FFT'd. This effectively produces slope ζ equivalent to

$$\zeta(x) = \frac{D(x+10) - D(x-10)}{20} \quad , \tag{1}$$

where D is draft, x is horizontal distance, and all units are metres. Individual data tests confirmed the equivalence (as did a full slope histogram comparison). The Gaussian smoothing function $G(k)$, in transform space, was

$$G(k) = e^{-17.77k^2} \quad , \tag{2}$$

and here the units of k are radians/m.

This is basically a simplified version of the criterion used in analyses by other researchers (see Wadhams 1981). The criterion used by Wadhams and Horne (1980) uses the same slope magnitude, but it incorporates different smoothing (their D1 criterion). In that criterion ice is "level" at point x metres if

$$|D(x+10)-D(x)| \leq 0.25\text{m} \quad \text{or} \quad |D(x-10)-D(x)| \leq 0.25\text{m}. \tag{3}$$

The span of 20 m in the present criterion is used in order to incorporate the total range of 20 m used by Wadhams and Horne (although theirs ultimately uses 10 m and so it does less smoothing and hence is more restrictive).

Some examples of data sequences so selected are shown in Figure 1. Here the segment in (a) from about 500 m to 3600 m looks like one long pan, but the criterion selects it as 5 pans

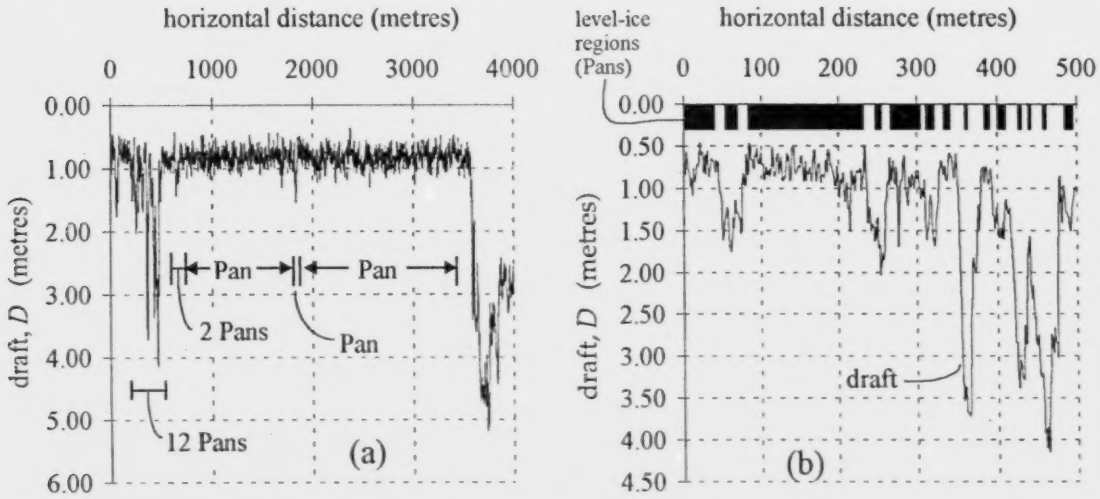

Figure 1. Examples of selected pans: (a) a segment showing two nearly contiguous long pans and many shorter ones; (b) the leftmost 500 metres in (a) with an expanded horizontal scale and with the pan locations indicated near the top axis.

because of local slopes outside of the 0.025 value. Two of these large local slopes are visible, near 630 m and 1840 m. The expanded view in (b) shows selected pan regions in greater detail. Most of the selected pans are in population 4 ice but some towards the 500 m edge are in higher draft peaks. By way of comparison, an analysis using the Wadhams and Horne (1980) slope criterion produces 83 pans in the 500-to-3600 m region of (a).

Only pans with lengths ≥ 15 m have been retained because shorter pans are heavily influenced by the 20-m span in the slope definition and because even a single population will exhibit short segments when analyzed in this fashion. Also, at 15 m the distribution of pan lengths from the *Gurnard* set begins to differ appreciably from the distribution of lengths from a computer-generated lognormal data set. The number of pans satisfying this length restriction for the *Gurnard* data is 8,752 (without it the number is 33,467). In Figure 1(b), only 4 pans have length ≥ 15 m, the 3 leftmost ones and the pan at 300 m.

For the present work, a further simplifying assumption is made, namely, that all of the ice in a given pan comes from one population. This is largely justified by an examination of the running means of ln(*Draft*) data within the pans, i.e. with the noise removed by the Gaussian filter of Eq. (2), which shows that 76% or more of the pans in each population satisfy this assumption for all of their smoothed data values. As well, many of the remaining pans are near ice draft population "boundaries" but are without anomalous standard deviations, so there seems to be no *a priori* reason to treat them as comprising composite populations.

The ice population categories are actually defined in terms of their mean values in the logarithmic domain, i.e. the means of ln(*Draft*). The ranges have been chosen to correspond closely to minima in the pdf's of draft and of level ice, and for each ice population they are given in Table 2 along with the number of pans in each range.

Table 2. Ranges of the Means, and Number of Pans in each Range

population	lower mean (log)	upper mean (log)	number of pans
5	-∞	-0.37	107
4	-0.37	0.2	196
3	0.2	0.85	2010
2	0.85	∞	6439

The probability density for the level-ice drafts is shown in Figure 2, and this function compares very well with a corresponding estimate for the same data given in Wadhams and Horne (1980) (their Figure 8 but mislabeled as Figure 5). The present estimate does show some differences from the Wadhams and Horne figure, mainly in the widths of their very narrow peaks, but the main features are very similar. Perhaps the lack of detailed identity is due to the different ways in which "slope" is numerically defined.

3. SPECTRA AND CORRELATION FUNCTIONS

A part of the subsequent analysis pertaining to the pdf will require an estimate of the

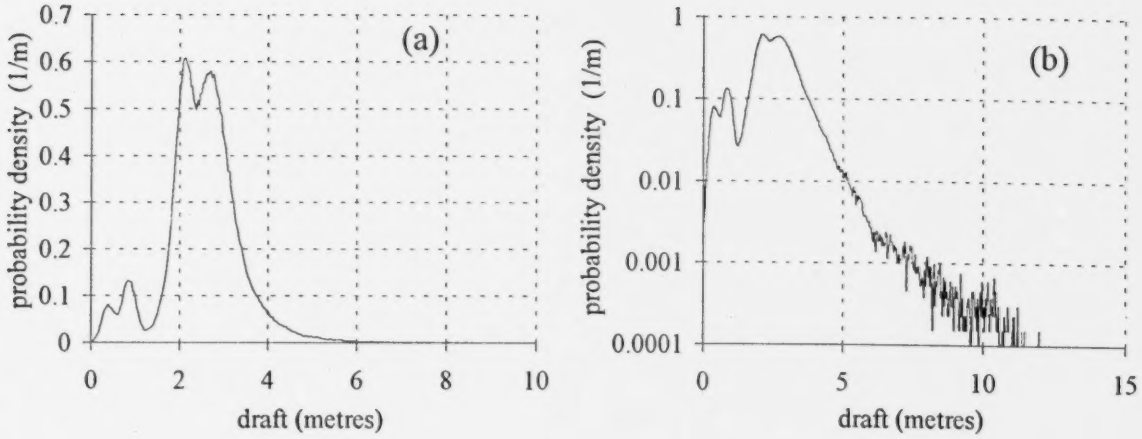

Figure 2. Probability density function for the level-ice drafts: (a) linear vertical scale showing clearly the multipeak structure; (b) logarithmic vertical scale showing extended exponential-like regions towards the large draft values.

correlation function for the 1-m spaced draft values. It is straightforwardly determined from the draft wavenumber spectra.

In the level-ice set the segment lengths range from 1 m to 1714 m. Draft spectra for ice populations 3 to 5 were produced for those segments with lengths ≥ 512 m, of which there were 26, and for ice population 2 for segments with lengths ≥ 256 m, again of which there were 26. They consistently show a lower "floor" with a Gaussian taper towards large wavenumbers (k) and with a root-mean-square value of 0.10 m. This is in essential agreement with the 9-cm noise level reported by Wadhams and Horne (1980). The spectral shape is shown in Figure 3 where an average of the 5 smallest-variance level-ice segments (with lengths ≥ 512 m) is shown along with an average of the 5 largest-variance level-ice segments (again with lengths ≥ 512 m). It can be seen that there is a common portion with wavenumbers > ~0.1 cycles/m. This feature is seen in all the spectra for the level-ice data. For comparison the spectrum for the entire Gurnard data set is also shown for wavenumbers between 0.1 and 0.5 cycles/m, and even in it there is a slight bulge apparent in this same range of wavenumbers.

The overall noise spectrum N, fitted to this common shape, is given approximately by

$$N = 0.045\, e^{-k^2/0.275^2} \qquad \text{m}^2/\text{cpm}. \qquad (4)$$

where the units of k are cycles/m. Estimates from each ice population provide this same form but

with slight differences in the parameters, as given below.

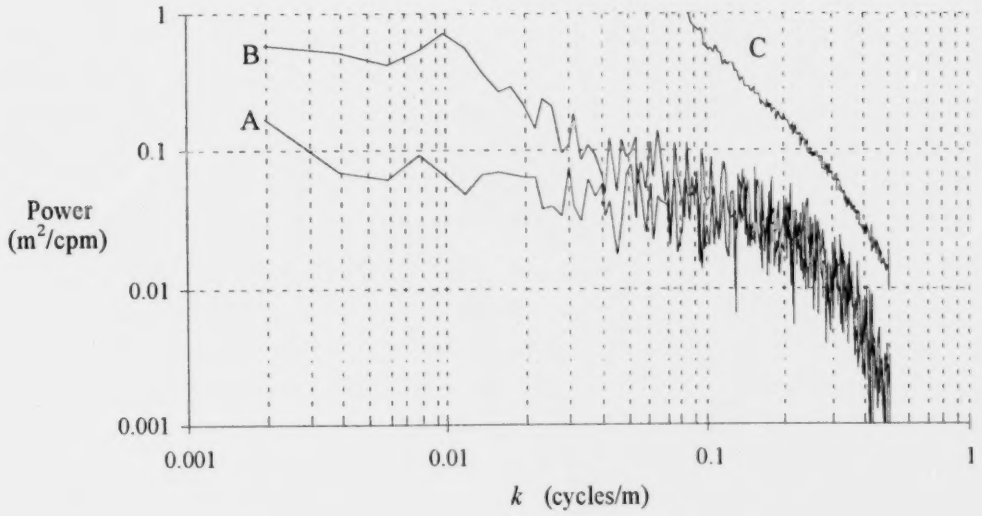

Figure 3. Spectra of level-ice segments. A) average of 5 smallest-variance segments with length ≥ 512 m; B) average of 5 largest-variance segments with length > 512 m; C) entire Gurnard data set.

The *non-noise* spectral shape I, i.e. the spectrum of the ice itself, is conjectured to be

$$I = \frac{0.0015}{(1+10000k^2)\sqrt{k}} \rightarrow \frac{0.045}{(1+500k^2)\sqrt{k}} \quad \text{m}^2/\text{cpm}, \qquad (5)$$

with the left formula pertaining to the smaller-mean pans and the right formula to the larger-mean pans. This form is postulated because it is similar to the overall draft spectrum shape as given previously for the *Gurnard* data (Hughes 1991). It implies that the short scales (large k-values) of the ice have a fractal dimension of 1.25, a value that is within the range given by Key and McLaren (1991) for scales of 3-15 m for a different data set (the taper towards a less steep slope as $k \rightarrow 0$ is also in agreement with their results), but it is significantly smaller than the value of 1.5 given by Melling and Riedel (1995) for first year and for "old" ice, also from a different data set. Their observation that the dimension is apparently independent of ice type implies that a single asymptotic drop-off in the spectrum with increasing k is valid and serves to justify the use of a single formula to describe the spectra. Their value of 1.5, however, would imply a k^{-2} behaviour instead of the $k^{-2.5}$ adopted here. The present shape is based on the full *Gurnard* spectral shape

for scales between 10 and 100 m in length. For scales < 10 m spectral portions do exhibit k^{-2} behaviour, but with other behaviours as well, ones that are possibly linked to measurement characteristics such as smoothing and noise. Because of this and because the present study is limited to the *Gurnard* data, the $k^{-2.5}$ behaviour is chosen.

The average of ice population 4 and 5 data shows a very good fit to

$$I + N = \frac{0.0085}{(1+2500k^2)\sqrt{k}} + 0.05e^{-k^2/0.26^2} \quad \text{m}^2/\text{cpm}, \tag{6}$$

giving a noise root-mean-square of 0.107 m, i.e. slightly higher than that above. The data and this curve are shown in Figure 4. The broken lines show separately the first and second terms in Eq. (6), i.e. the ice portion (I) and the noise portion (N), respectively.

Spectra of the log domain data, i.e. ln(D), show similar shapes (except for the entire set) but not with such a simple division in level.

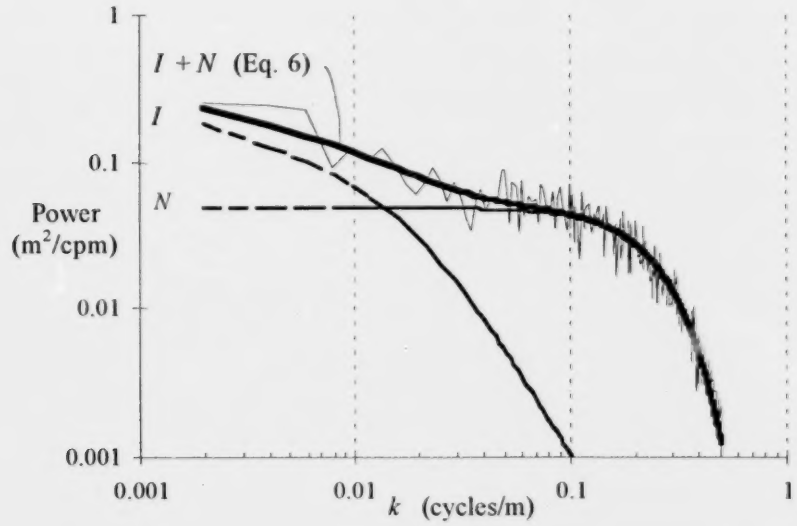

Figure 4. Ice population 4 & 5 draft spectra. The data (light line) are a spectral average of 16 segments, each with 512 samples. The fitted curve (Eq. (6)) is shown as the heavy line, and the two individual portions (Ice and Noise) are shown separately as broken lines.

Formulae for the spectral shapes are summarized in Eq. (7), with the parameters for the relevant cases shown in Table 3,

$$I+N=\frac{A}{\left\{1+\left(\frac{k}{\beta}\right)^2\right\}\sqrt{2\pi k}}+\frac{B}{2\pi}e^{-\left(\frac{k}{\beta_0}\right)^2} \tag{7}$$

and where the units are m^2/(rad/m) for $I+N$ for the linear domain, 1/(rad/m) for $I+N$ for the log domain, and rad/m for k for both domains.

Correlation functions, $C(n)$, where needed can be computed by Fourier cosine transforms of the above spectra, i.e. $(I+N)$. The transform integrals can be evaluated analytically, and for the general form of Eq. (7) the resulting function is as follows:

$$C(n)=\frac{\frac{A\sqrt{\pi\beta}}{4}\left\{e^{n\beta}\mathrm{erfc}(\sqrt{n\beta})+e^{-n\beta}[1+\mathrm{ierf}(-i\sqrt{n\beta})]\right\}+\frac{B\beta_o}{4\sqrt{\pi}}e^{-\left(\frac{n\beta_o}{2}\right)^2}}{\frac{A\sqrt{\pi\beta}}{2}+\frac{B\beta_o}{4\sqrt{\pi}}} \tag{8}$$

(Note that $i$erf($-ix$) is a real function of x.) $C(n)$ has also been computed from the actual data sets by lagged products for some cases, and the correspondence between the results of the two methods is quite satisfactory.

Table 3. Spectral Parameters

Domain	population	A	B	$\beta/2\pi$	$\beta_0/2\pi$
linear	5	0.0015	0.045	0.01	0.275
linear	5 & 4	0.0085	0.05	0.02	0.26
linear	3	0.025	0.045	0.02	0.275
linear	2	0.045	0.0375	0.04472...	0.285
linear	all*	26.1328	0.07	0.009	0.275
log	5	0.08	0.35	0.025	0.28
log	4	0.007	0.065	0.025	0.27
log	3	0.004	0.011	0.03333..	0.275
log	2	0.00675	0.0055	0.04472...	0.285
log	all**	0.6788	0.025	0.009	0.28

*the value for B also includes effects other than the noise, possibly interspersed pan means.

**includes a term ~$0.225\exp(-13.5\sqrt{k})/k^{3/4}$ (cpm) probably due to interspersed pan means.

4. CONVOLUTION MODEL

The full equation for the pdf of draft D for the convolution model is

$$\text{pdf}(D) = \sum_i \alpha_i \int_0^\infty \int_0^\infty \int_{-\infty}^\infty \text{jpdf}_i(n,\sigma,\mu) \frac{e^{-\{\ln(D)-\mu\}^2/2\sigma^2}}{\sqrt{2\pi}\,\sigma\, D} d\mu\, d\sigma\, dn \qquad (9)$$

where jpdf_i is the joint probability density function pertaining to the i^{th} ice population, and it is shown as a function of the pan length n, pan standard deviation σ, and pan mean μ, with the last two pertaining to drafts (D) in the log-domain (for calculations done in the linear domain the kernel in Eq. (9) is a Gaussian rather than the lognormal as shown).

The probability density of level-ice draft (Figure 2) shows the typical "exponential tail" portions for large drafts similar to the full draft pdf as shown in Hughes (1991), Figure 1b, (and by many others) thus indicating that the lognormal approach is appropriate—especially for the larger draft (population 2) data between 3 and 6 m for the level ice and for larger draft values as well, although in the figure these may be too strongly contaminated by deformed ice values to be indicative of level-ice behaviour. Melling and Riedel (1996a & b) also provide observational evidence of pack-ice draft standard deviations being proportional to the mean when deformed ice is included, a result that is strongly suggestive of lognormality at least for the larger drafts. As well, Key and McLaren (1991) provide clear evidence of this same effect for a data length of 3000 km and drafts with mean values ranging from less than 2 m to greater than 4 m. The other ice draft populations in the present study (3 to 5) are all narrow enough for either the normal or lognormal shape to be assumed with little difference between them.

The derived estimates for μ and σ generally display low correlations (within ice-populations) in both the log-domain and the linear domain. Correlation values for populations 2 to 4 are ~0.4 (or less) for the linear data, and -0.3 (or nearer zero) for the log data. The population-5 μ and σ estimates show a similar correlation magnitude (~0.5) for log- as for linear-data. For the present accuracy, these correlations are not considered significant enough to warrant their inclusion in the model.

Thus the analysis so far indicates that lognormality is supported as a suitable modelling basis—mainly because of its better fit for the larger draft regions where the distinction between normal and lognormal becomes more pronounced—and that a satisfactory model for jpdf_i (at this level of accuracy) is simply a product of three independent pdf's, one each for n, σ, and μ. The following three subsections provide estimates for these 3 pdf's.

4.1 Pan Lengths

The distributions of the run lengths for pans within the various ice populations (not including ice population 1) were determined assuming that they were approximately lognormal. *All* of the pan data were used here, including those with lengths < 15 m.

Histograms of ln(n) were constructed for data within each ice population draft range, and they characteristically have two peaks. These were fitted manually by lognormals, and the interpretation is that one of them—for the shorter segment lengths—represents the background data (i.e. data that would be obtained from a lognormal draft distribution even without different population pans being interspersed throughout), and the other—for the longer segment lengths—represents the distribution of the interspersed pans themselves. The curves obtained for ice population 5 data and population 3 data are shown in Figure 5. The leftmost peak in the data-values and the leftward portion of each heavy line represent the "background" segments, and the

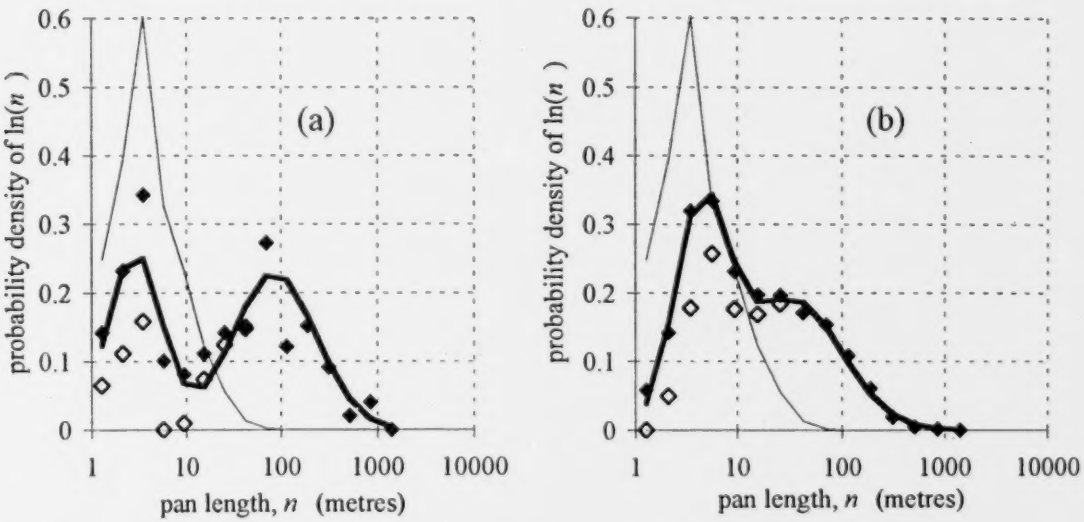

Figure 5. Probability density of ln(n). (a) ice population 5; (b) ice population 3. Measured data (♦), measured data with "background" segment histograms subtracted (◊), two lognormals fitted (heavy line), simulated single population pdf (light line).

peak (or plateau) toward the right represents the pans. A numerically simulated single-population curve based on ice population 1 parameters has been determined as an estimate of the background segments, and a suitably scaled version of this has been subtracted from the measured data values (without totally eliminating the leftward peaks) and is also shown for comparison. Fitted lognormal parameters for the pan-portion only for each of the ice populations are given in Table 4. These are defined in accordance with the following standard formula:

$$\text{pdf}(n) = \frac{e^{-\{\ln(n)-M_n\}^2 / 2\sigma_n^2}}{\sqrt{2\pi} \cdot s_n \cdot n} , \qquad (10)$$

with $\langle length \rangle \equiv \langle n \rangle = e^{(M_n + 0.5\sigma_n^2)}$.

Ice population 5 provides the clearest separation between the "background" and the pans, and it also displays the largest M_n-value and hence the longest pans. The separation and the M_n-values gradually reduce on progressing toward larger draft populations until for population 2 the mean length is only 36.78 m and the separation is even less apparent than that shown in Figure 5b. Nevertheless, the longer pans in ice populations 2 and 3, i.e. $n > 50$ m, do display probability density curves that are relatively uncontaminated, and thus the M_n-values and this reducing trend do have some reliability. Calculations using a wider slope criterion, i.e. $|\text{slope}| \leq 0.075$ instead of 0.025, provide similar results but with the M_n's being more constant over the ice populations (with values similar to that given above for population 5). However it is possible that this criterion overdoes the amalgamation of neighbouring level-ice regions by ignoring interspersed areas that are more properly categorized as deformed ice. As an example of its greater amalgamation tendency, in the data displayed in Figure 1, the five pans in the 500-to-3600 m region in (a)

Table 4. Parameters for Probability Density of Pan Length

Population	M_n	σ_n	<length> (m)
5	4.45	1	141.17
4	3.75	1	70.11
3	3.5	1.1	60.64
2	3	1.1	36.78

are consolidated into one pan, and the 14 pans in (b) are reduced to 6. (The Wadhams and Horne method using this wider 0.075-value also consolidates this region in (a) into one pan.)

4.2 Standard Deviations

For the present analysis the pan data set was examined to determine whether the standard deviations of the pans (log or non-log) were statistically uniform within each of the basic pdf ice populations. Because the pan lengths represent particular sample sizes "drawn," as it were, from a single population, the calculated standard deviations (and means) for these samples will display random sample-to-sample variations even though the population parameters for each sample, i.e. each pan, are the same. The magnitude of this sampling variation depends inversely on the

sample size—in particular, on the number of statistically independent points there are in each sample (pan). As shown in Figure 3 and Figure 4, the spectrum of the ice draft data within each pan is not flat, thus the data points are correlated. To allow for the effects of this correlation, there are two available methods: (i) decorrelate the original data sequences and then use standard tests devised for uncorrelated data; (ii) determine the dependence of the statistical parameters on the correlation function of the underlying data and use the form of that dependence instead of the standard test. It is the latter method that has been used here.

With M and s as the arithmetic mean and standard deviation of the draft (log or non-log) in each pan respectively, and C_k as the correlation between draft values separated by k metres, it is shown straightforwardly in the Appendix that

$$\begin{aligned}\sigma_M^2 &= \frac{\sigma_s^2}{n^2}\sum_{k=-n+1}^{n-1}(n-|k|)C_k \\ &= \sigma_s^2\{\frac{1}{n}+\frac{2}{n^2}\sum_{k=1}^{n}(n-k)C_k\} \\ &= \sigma_s^2\{\frac{1}{n}+\frac{2S_n}{n}-\frac{2T_n}{n^2}\} \equiv \frac{\sigma_s^2}{l_M(n)}\end{aligned} \tag{11}$$

$$\mathrm{var}(s^2) = \frac{\sigma_s^4}{l_s(n)} \quad , \tag{12}$$

where σ_s^2 is the variance of the draft data and l_M and l_s are measures of the number of independent points in the pan. These last two are monotonically increasing functions of n, and are straightforwardly determinable but are algebraically quite complicated (l_s here is the same as l_3 in the Appendix). If the data were uncorrelated, l_M and l_s would be simply n, and $n^2/2(n\text{-}1)$, respectively. For the correlated data, l_M and l_s require numerical evaluation using the correlation functions obtained from the spectra (for each ice population). Representative values are given in Table 5 for data from ice population 5. It can be seen that the correlation significantly reduces the

Table 5. Number of Independent Points

Pan length n (m)	l_M	l_S
20	4.0	11.0
100	9.4	32.6
1000	41.6	202.1

effective number of independent points compared to the total number of data points in the sample. Ice population 4 values are quite similar, and ice population 3 and 2 values are even more strongly reduced for the larger pan lengths.

The calculated standard deviation s-values from the actual level-ice pans were plotted against n for each ice population. Results for ice populations 5, 4, and 3 are shown in Figure 6 (there are too many data points in ice population 2 to present them this way). Here log-draft versions are shown, along with the linear draft version for the combined 4 and 5 ice population data sets. The depicted values show a marked reduction in the spread of s with increasing n very much in accordance with formulae of Eqs. (11) and (12). The vertical widths of the scatter are shown as functions of n in the panels immediately below each scattergram. Here the width is measured by q, where

$$q = \text{std dev } \{\ln(s^2)\} \ . \tag{13}$$

Along with the individual data points (•) the light line in each panel assumes a δ-like distribution for σ, and the heavy line assumes a lognormal distribution with a standard deviation (τ) value of 0.6 for ice population 5, 0.3 for ice population 4, 0.3 for ice population 3, and 0.25 for ice populations 4 and 5 linear. (A δ-distribution and a lognormal distribution in σ both result in a closely lognormal distribution for s, as has been determined by numerical simulations.)

It is apparent that the lognormal distribution ($\tau \neq 0$) fits the q-value data better than the δ distribution ($\tau = 0$), and thus that there is more than just sampling effects producing the spread in s-values. However, for all but ice population 5, the q-values for large n's are quite small, < 0.35, indicating that σ^2 varies by $\sim \pm 35\%$, and thus σ by only $\sim \pm 17.5\%$. For the smaller n's the measured values all tend to be larger than the predictions, perhaps due to the influence of some improper inclusion in the samples of ice population 1 values (the deformed ice) which are more highly correlated from point-to-point than those from other ice populations and which thus would produce larger standard deviations, or due to some end effects in the filtering inherent in the pan-defining slope field which would represent a few (possibly large) erroneous values to be included in the calculations of s. As n increases both of these effects would decrease and so strongest reliance is put on the larger n-value results. From these the standard deviations of $\ln(s^2)$ all appear to be sufficiently low that, to at least a first approximation for modelling purposes, σ can be taken to be independent of n, and originating from a single underlying value for each ice population.

Population 5 data display larger q-values, but it can be seen that a large proportion of this comes from variations that are correlated with the means. The open circle (o) data in Figure 6a have a larger mean than the solid symbol (♦) data (see next section). This is possibly due to the effect of working in the log domain on the (linear) high frequency measurement noise

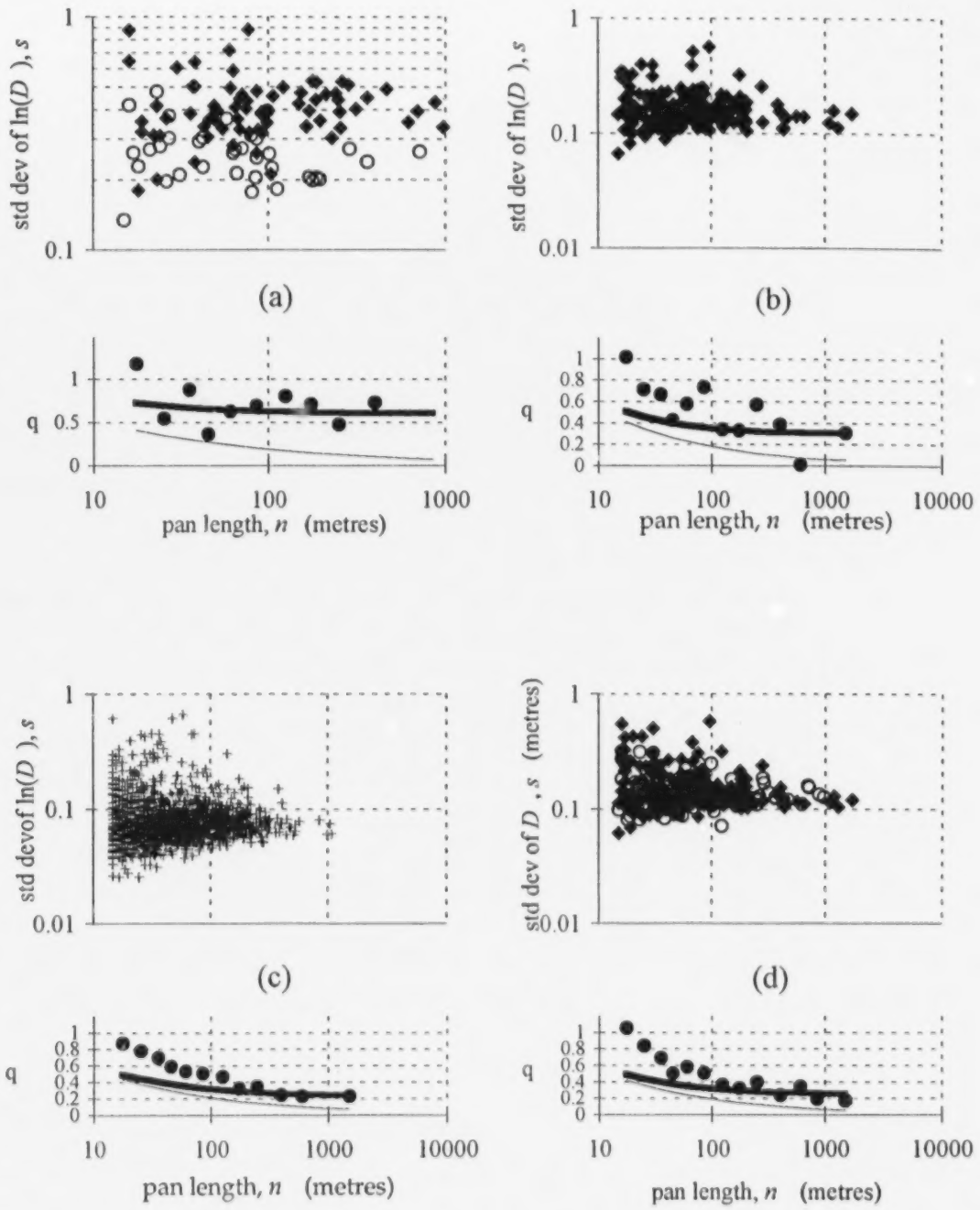

Figure 6. Standard deviation (s) as a function of pan length (n). The decrease in the range of s-values as n increases is strongly apparent. q-values (standard deviation of $\ln(s^2)$) for these data are shown by the symbols (•) in the panels immediately below each scattergram. q-values from the sampling model are shown by the solid lines: τ=0, light line; $\tau\neq0$ heavy line. (a) ice population 5, log-data, 5a (o), 5b (♦)_as referred to later in the text, τ=0.6; (b) ice population 4, log-data, τ=0.3; (c) ice population 3, log-data, τ=0.3; (d) ice population 4 (♦) and 5 (o) combined, linear data, τ=0.25. Note the logarithmic axes on all but q.

component—the logarithm effectively dividing the standard deviation of the noise by the local mean, thus separating it where the means are identifiably separate. If these two sets were not separated τ would be significantly reduced. Certainly for the linear domain population 5 data, the large n's do display small q-values (~0.2), as can be seen in Figure 6d.

An example of the distribution of s^2 for ice population 2 for pan lengths between 70 m and 100 m is shown in Figure 7a (using a logarithmic s^2 axis) and it can be seen that the lognormal form for σ fits the data very well. From Figure 7b it can be seen that the heavy line (τ=0.35) fits the Wadhams and Horne q-values essentially over all the represented n's—and this trend is consistently displayed in the other ice populations as well. Also shown are values obtained from the 0.075-criterion and these all tend to be larger than either the 0.025 q-values or the Wadhams and Horne q-values and they deviate more strongly from the predictions. Even so, for large n's they are again only ~0.5 which is not large.

Finally, the effect on pdf(D) of a non-zero width for pdf(σ^2) has been exam ined using

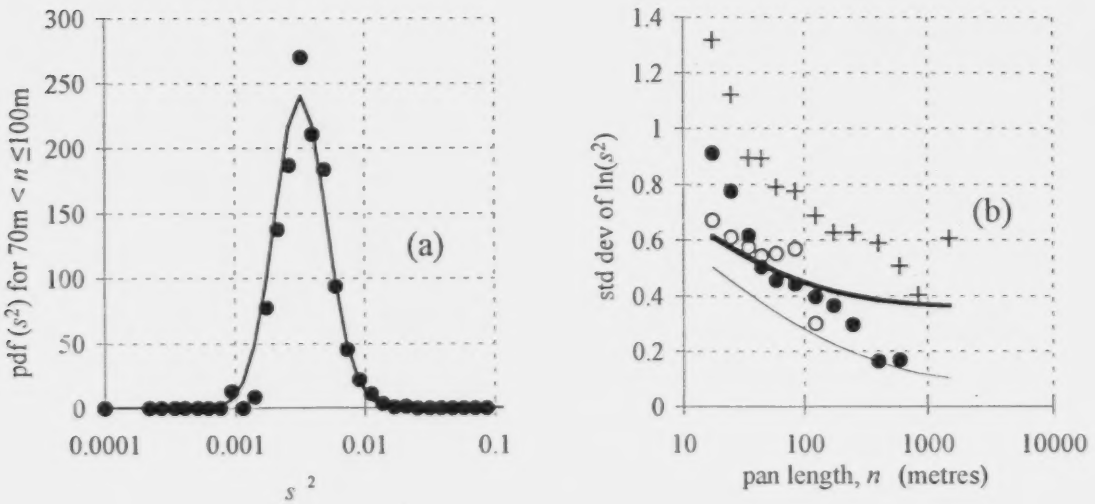

Figure 7. Ice population 2 comparisons: (a) Pdf(s^2) for pan lengths between 70 m and 100 m, measured data (•), lognormal form with τ=0.35 (line); (b) standard deviation of ln(s^2) showing measured values using the Wadhams and Horne criterion (o), the present method (•), the present method with a slope criterion of 0.075 (+), τ=0 (light line), τ=0.35 (heavy line).

numerical simulations. The lognormal form is not convenient for this, however an Inverse Gaussian formulation, i.e. $\text{pdf}(\sigma^2)=\{\sigma_0/\sigma^3\tau(2\pi)^{1/2}\}\exp\{-([\sigma^2-\sigma_0^2]/2\sigma_0\tau\sigma)^2\}$, is very similar in shape and can be treated by Fourier transforms (and ultimately evaluated with an FFT) and so it has been used instead. With τ=0.4, the result is that its effect on pdf(D) is insignificant for all but

ice populations 4 and 5, and even for those it produces deviations of < 5% for pdf's that have any significant value, i.e. pdf > 0.0005 m^{-1}. For pdf's less than this—and they occur only for D < 0.16 m—the proportionate change is larger than 5% but the pdf's in this range are unimportantly small. Even for τ=0.6, the value for ice population 5 (uncorrected), the maximum deviations rise only to 9%, with all else remaining the same.

Thus, it can be seen that variations in the standard deviation estimates are due in large part to simple sampling variations, and that, to the present degree of accuracy in the method of selecting the pans, a model that assumes a constant standard deviation within each draft pdf peak is not an unreasonable first approximation. With this model the pdf's of standard deviation become, quite simply, δ-functions.

Estimates for a single standard deviation-value σ_S for each ice population have been obtained from the large-n regions of the s-data, i.e. where the range in s-values—the q's—are quite small. These final estimates are given in Table 6.

Table 6. Standard Deviation Values

population	σ_S (log)	σ_S (non-log), m
5	0.35	0.1125
4	0.125	0.1125
3	0.068	0.14
2	0.0625	0.16

4.3 Means

From the complete set of data, it is generally apparent that the degree of scatter in M is too large to be accounted for solely by sampling effects. Some decreasing trend of the scatter of M with increasing n is evident, as shown in Figure 8 for ice populations 4 and 5, but only 41% of the data values are within the 95% confidence lines for population 4, and 36% are within for population 5. Here the confidence limits are estimated as functions of n assuming that pdf(M)—the M-portion of $jpdf_i$—is Gaussian as given by Eq. (14) i.e. assuming the μ-dependence in $jpdf_i$ to be a δ-function. If μ were indeed δ-like, so that *all* of the scatter were due to sampling effects, there ought to be approximately 95% of the data values included between these confidence lines, but because 41% and 36% are so much smaller that 95%, the implication is that μ takes on more than one value, perhaps a range of values. It is evident in Figure 8a that ice population 5 comprises two relatively distinct populations, populations 5a and 5b say, each of which displays only sampling scatter in M, i.e. each of which is satisfactorily represented by a δ-function in μ-space. One (5a) is an elongated horizontal cluster with M-values of very nearly -

0.5, the other (5b) is a larger cluster with M-values of very nearly -1.02, as indicated in the figure. The 95% lines as shown quite easily encompass ~90% of the data in either of these clusters by themselves if the lines are shifted vertically to centre on either of these M-values (but without altering the lines' separation) and so there is perhaps some justification for considering ice population 5 to be not a continuous Gaussian distribution in μ-space, but a simple 2 component discrete distribution—at least for the present data set. (As discussed earlier the standard deviations for population 5 also separate out somewhat into two sets as can be seen in Figure 6a where the open circles (o) pertain to ice population 5a and the solid symbols (♦) to ice population 5b. The σ_S-value of 0.35 as given in Table 6 becomes 0.27 for 5a and 0.37 for 5b.) The scatter presented by ice population 4 indicates for it a more continuous form for the distribution of μ.

Also, μ and n are essentially uncorrelated within each ice population (estimates provide correlations of -0.27 for ice population 2, and < 0.1 in magnitude for the others).

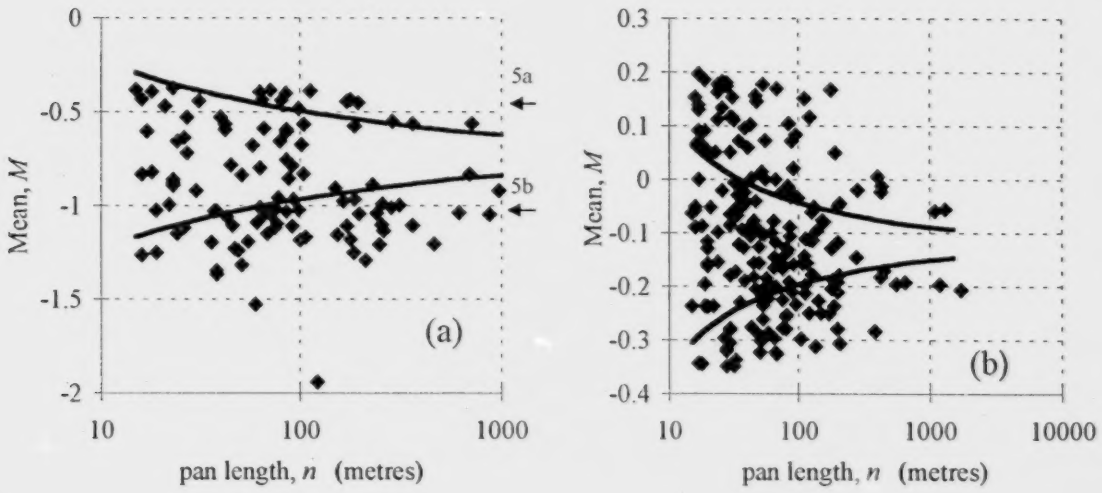

Figure 8. Mean-values (M) as a function of pan length (n). Data points are shown as symbols (♦), and 95 percentiles as solid lines assuming pdf(μ) is a δ-function: (a) ice population 5; (b) ice population 4. Note the logarithmic n-axis.

The final overall estimate for the pdf(M) is contained in the histogram-curves as shown in Figure 9. Here the data and the curves are counts of the number of values in each bin, with a bin width of 0.05. The curves are sums of normals—one for each ice population—and the parameters defining them are obtained by starting with the smoothly fitted curves for pdf(D) and algebraically deleting the effect of the (δ-function) standard deviation values and the average pan lengths. (In the log-D domain these curves are all normals so this algebraic process is merely the

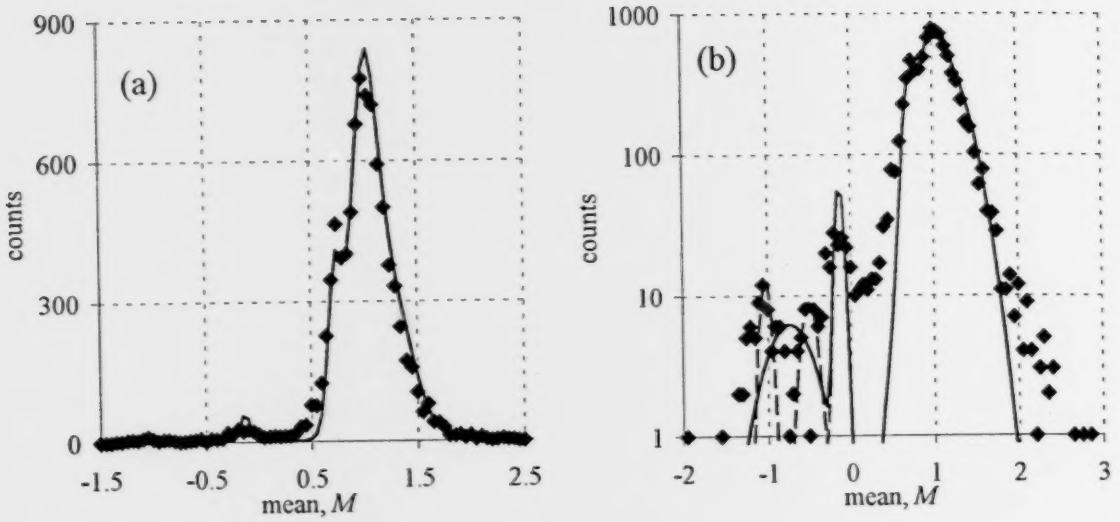

Figure 9. Distribution of the pan means (M). The symbols (♦) indicate the measured data, and the solid and broken lines indicate the fitted curves. (a) linear vertical scale showing the fit near the large peaks; (b) logarithmic vertical scale showing the fit near the smaller values.

manipulation of Gaussians which is very straightforward, and in fact becomes simply the subtraction of the relevant variances.) It can be seen that this yields a fit to the measured histogram of M that is quite satisfactory for this method of defining the pans. It also has the virtue that it guarantees recovery of the fitted pdf(D) curves.

The single Gaussian peak for ice population 5 is shown as a solid line (Figure 9b, $M < -0.37$) and it can be seen that this single peak fits the data only approximately well. With the 2-component discrete approach of population 5a and 5b (broken lines), the smooth curve for M does fit the data very much better. (The peaks in the curves representing ice populations 5a and 5b have been given a non-zero width for plotting purposes, and the width has been chosen so that the height is about the same as the data points.) However, notwithstanding this improved fit in M-space, the resulting fit to the final pdf(D) is not as good with the discrete two components as it is with the single Gaussian. In order to use the α-values pertaining to the draft pdf in fitting the displayed lines it is necessary to allow for different average pan lengths in each of the different ice populations. This has been done for the curves in this figure by simply dividing the relevant α-value by the average pan length as given in Table 4 (and then normalizing by the sum of all the relevant α's weighted in this fashion).

It should be noted that the data-values displayed in Figure 9 represent *sampled* statistics, but the smooth curves represent *population* statistics. Because the sampling effects broaden any

peaks in the distributions—with the broadening effect increasing as the pan length decreases, in accordance with Eq. (11)—it is perhaps not surprising that the measured data display generally broader peaks than the smooth curves (particularly for the narrower peaks).

The final parameters for the normals for M are given in Table 7, and the standard Gaussian form

$$\text{pdf}(M) = \frac{e^{-(M-m)^2/2\sigma_m^2}}{\sqrt{2\pi}\,\sigma_m} \tag{14}$$

is used for each ice population. As part of the process for obtaining these a refitting of all the basic pdf parameters was done similar to the description given by *Hughes*, (1991) but using a least-mean-square numerical fitting process and fitting for 6 peaks only. The resulting values are thus somewhat different from those previously published. The σ_m-values are the square-roots of the differences between the squares of the σ-values obtained from the refitting process and the corresponding σ_s-values given above in Table 6, except for ice populations 5a and 5b as described above. It is worth emphasizing that the curves in Figure 9 are not fitted directly to the data in

Table 7. Gaussian Parameters for the Means

population	m	σ_m
5b	-1.02	0
5a	-0.5	0
5	-0.73	0.258
4	-0.1283	0.0468
3	0.7405	0.068
2b	1.0225	0.113
2a	1.1696	0.230

the figure. The curves are defined by parameters fitted to data-values which pertain to other variables, namely draft, pan standard deviation, and average pan length. This lends additional support to the adequacy of the fit, and some encouragement to the entire process.

4.4 Final Pdf

With n, μ and σ uncorrelated, σ δ-like at $\sigma=\sigma_s$, and μ Gaussian as in Eq. (14), the three integrals in Eq. (9) can be evaluated and the result for each ice population i is simply

$$\text{pdf}(D) = \alpha \frac{e^{-\{\ln(D)-m\}^2/2\{\sigma_m^2+\sigma_s^2\}}}{D\sqrt{2\pi\{\sigma_m^2+\sigma_s^2\}}} \qquad (15)$$

The total pdf(D) is the sum of these over all i, with α, m, σ_m and σ_s understood to have i-subscripts. A summary of all the values for these parameters based on the present analysis is given in Table 8.

Table 8. Pdf Parameters for all the Populations

population	α	m	σ_m	σ_s	$\sigma=\{\sigma_m^2+\sigma_s^2\}^{1/2}$
5	0.017	-0.73	0.258	0.35	0.435
4	0.0149603	-0.128284	0.0468	0.125	0.1334926
3	0.09612	0.740463	0.068	0.068	0.096327
2b	0.15689	1.02247	0.113	0.0625	0.129235
2a	0.25713	1.16958	0.230	0.0625	0.238434
1	0.4631	1.42229	0.0	0.560238	0.560238

5. ESTIMATED DRAFT PROBABILITY DENSITY WITH THE NOISE REMOVED

Although Wadhams and Horne (1980) claim that the "high-frequency noise" will "not have a serious effect on the probability densities of draft," its pdf does convolve the entire pdf of draft thus effectively broadening all the peaks. To be sure, this is not a serious effect unless the peaks have a width that is comparable with the root-mean-square value of the noise itself, i.e. ~0.1 m. However, this *is* the case for the smaller draft peaks (ice populations 5, 4 and 3, and possibly even 2b).

This noise component is essentially Gaussian and can be included in the pdf description as a convolution, so that for each population

$$\text{pdf}(D) = \alpha \int_o^\infty \frac{e^{-(D-D')^2/2\sigma_{noise}^2}}{\sqrt{2\pi}\,\sigma_{noise}} \frac{e^{-(\ln(D')-m)^2/2(\sigma_m^2+\sigma_s^2)}}{\sqrt{2\pi(\sigma_m^2+\sigma_s^2)}\,D'} dD' \qquad (16)$$

where the σ_m and σ_s are the standard deviation of the (log) means of the segments and the (log) ice draft within the segments, respectively, and α is the proportion of total field represented by that ice population. The final pdf is the sum of these over all ice draft populations. Two methods have been used in an attempt to determine the parameters m and $(\sigma_m^2+\sigma_s^2)$: the first is a simple

approximate method that calculates the mean and variance of D with and without the noise factor present, and equates the results; the second uses a Wiener filter.

5.1 Approximate Method

If pdf(D) is assumed to be lognormal (even with the noise corrupting the data) for each ice population, with shift and width parameters m and σ, then the mean and variance of D are

$$\langle D \rangle = e^{(m+0.5\sigma^2)},$$
$$\mathrm{var}(D) = e^{(2m+\sigma^2)}(e^{\sigma^2} - 1). \tag{17}$$

If the form of Eq. (16) is used, i.e. the noise is explicitly included, the mean and variance can straightforwardly be shown to take the following form—and here m_a and σ_a are shift and width parameters that pertain to the draft data in the absence of the noise:

$$\langle D \rangle = e^{(m_a+0.5\sigma_a^2)},$$
$$\mathrm{var}(D) = e^{(2m_a+\sigma_a^2)}(e^{\sigma_a^2} - 1) + \sigma_{noise}^2. \tag{18}$$

With the means from Eqs. (17) and (18) equated, and the variances similarly equated, m_a and σ_a can be calculated in terms of m, σ, and σ_{noise}. Numerical results, taking σ_{noise} to be 0.1 m, are given in Table 9 where m_a and σ_a are relabelled m and σ. The column second from the right represents "corrected" pan standard deviations, σ_s's, corrected assuming that all of the difference between the σ's in Table 8 and Table 9, i.e. all of the effect of the noise, appears in σ_s, and none in σ_m—a not unreasonable assumption. From the σ columns in these two tables it can be seen that very little change is made except for ice populations 4 and 5 for which the m's are slightly increased but for which the σ's are significantly reduced. By comparing the σ_s column in Table 9 with the σ_s column in Table 8 it can be seen that, except for ice population 5, the noise-reduced standard deviations are much more uniformly ~0.05.

5.2 Wiener Filter

In this technique, the full, measured pdf*(D)* is FFT'd and the transform is multiplied by the Wiener filter function *W(k)* and divided by the transform of the noise *R(k)*. The result is inverse-transformed by FFT, resampled to be uniform in the log-domain (and multiplied by D to make it basically Gaussians) and then subjected to the peak-fitting process. The resulting parameters are contained in Table 10. It should be noted that in Table 8 and Table 10 the α's have

not been constrained to sum to unity. For the "before" values $\Sigma\alpha = 1.0052003$, and for the "after" values $\Sigma\alpha = 1.001789$. (Also, the numerical peak-fitting process used here only allows 5 Gaussians and so ice population 5 was fitted manually using σ from Table 9.)

It can be seen that the σ_s column—which is produced here the same way as in Table 9, i.e. assuming no change in σ_m—does not present values that are so uniform as those in that table. In fact ice population 2b results in a σ-value that is less than σ_m and so the subtraction cannot be performed.

Table 9. Lognormal Parameters—Approximate Method for Noise Removal

population	m	σ_m	σ_s	σ
5	-0.7150	0.258	0.3045	0.399110
4	-0.12201	0.0468	0.0555	0.072591
3	0.74158	0.068	0.0492	0.08393
2b	1.023096	0.113	0.0518	0.124296
2a	1.17001	0.230	0.0556	0.236622
1	1.42245	0.0	0.559961	0.559961

Table 10. Lognormal Parameters—Wiener Filter Method

population	α	m	σ_m	σ_s	σ
5	0.017	-0.717	0.258	0.3045	0.3991
4	0.019779	-0.103387	0.0468	0.122	0.130347
3	0.06014	0.73902	0.068	0.0124	0.06912
2b	0.09527	1.03257	0.113	—	0.11129
2a	0.43011	1.08409	0.230	0.15712	0.278542
1	0.37949	1.52447	0.0	0.524868	0.524868

The Wiener filtering function W is given theoretically by (Press, et al. 1992, p. 548)

$$W(\kappa) = \frac{S(\kappa)}{S(\kappa) + P_n(\kappa)} , \tag{19}$$

where $S(\kappa)$ is the squared modulus of the transform of the measured pdf(D)—as estimated with the noisiness of the transform subtracted—and $P_n(\kappa)$ is the squared modulus of this noisiness. (This noisiness is not the same as the measurement noise that is being removed, instead it is associated with the bit noise and general inaccuracies inherent in the formation of the pdf itself.) $S(\kappa)$ is taken exactly as measured for $\kappa \leq 12.6825$ rad/m. For $12.6825 < \kappa \leq 65.2244$ it is taken as

$\exp(-0.01\ \kappa^2)$ times the $S(\kappa)$-function obtained from the 6-peak fitted smooth pdf, and for κ larger than this S is taken to be $\exp(-17.4686-0.0124\ \kappa^2)$. This fitting process for $S(\kappa)$ is necessary because for $\kappa > 16$, or so, $S(\kappa)$ as measured is essentially the noise field $P_n(\kappa)$, yet what is needed is an estimate of the uncontaminated $S(\kappa)$. The factor $\exp(-0.01\ \kappa^2)$ is necessary to provide a smooth fairing to the final exponential form for the largest κ range, and for convergence of the overall Wiener-filtering process. The final $S(\kappa)$-curve, and the portions just described, are shown in Figure 10. $P_n(\kappa)$ is taken to be the constant value $9.4234\ 10^{-7}$. These numerical values and trends were obtained graphically from the FFT of pdf(D) (obtained in the linear domain). Here the wavenumber κ pertains to the transform of the pdf and so it is conjugate to the draft D (not the horizontal spacing between samples as k is in the previous analysis). The filtering function $R(\kappa)$ is the transform of the measured noise being convolved "out," and with the Gaussian assumption it becomes

$$R(\kappa) = e^{-\sigma_{noise}^2 \kappa^3/2} \quad . \tag{20}$$

As before σ_{noise} is taken to be 0.1 m.

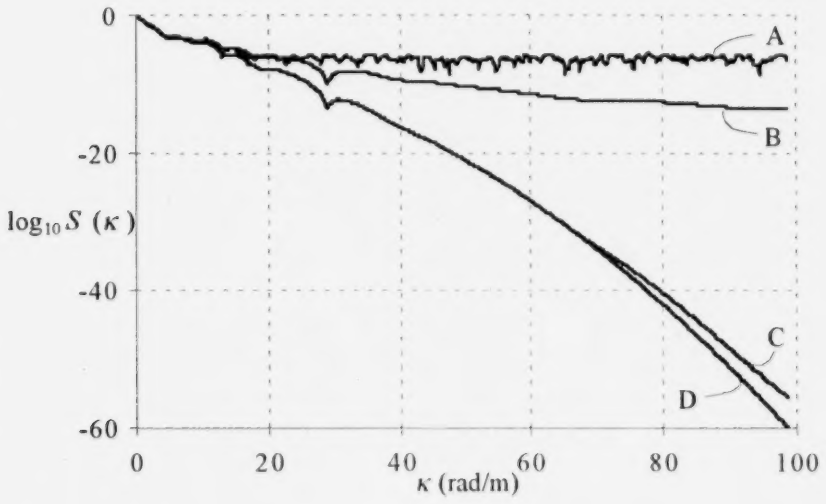

Figure 10. $S(\kappa)$ as used in the Wiener filter. Curve 'A' is the transform (squared) of the draft pdf, 'B' is the same for the fitted 6-peak lognormal sequence, 'C' is 'B' multiplied by $\exp(-0.01\ \kappa^2)$, and 'D' is 'C' with an extension of $\exp(-17.46-0.0124\kappa^2)$.

6. SLOPE DISTRIBUTION FUNCTION

Using the lognormal approach the probability density function (pdf) for drafts is given by

$$\text{pdf}(D) = \sum_i \alpha_i \frac{e^{-\{\ln(D)-m_i\}^2/2\ \sigma_i^2}}{\sqrt{2\pi}\ \sigma_i\ D} \tag{21}$$

where D is the draft value, m_i, σ_i and α_i are the mean, standard deviation and proportion of the i^{th} ice draft population. A further refinement—the convolution pdf model described above—allows the ice for a particular population to be contained in track segments (pans) which exhibit the same σ_i-value, σ_{si}, but which themselves display a range of mean-values within that population. In this case σ_i^2 for each population is replaced by $(\sigma_{mi}^2+\sigma_{si}^2)$ where σ_{mi} is the standard deviation of the mean-values for that population. (If the convolutional aspects of this model are not used, σ_{mi} is simply set to 0, and the equations and definitions transform and simplify in an obvious manner.) In the following the draft population subscript i is suppressed.

Slope ζ is defined as

$$\zeta(x) = \frac{D(x+\Delta/2) - D(x-\Delta/2)}{\Delta} \tag{22}$$

or,

$$\zeta(x) = \frac{e^{L_{x+\Delta/2}} - e^{L_{x-\Delta/2}}}{\Delta} \tag{23}$$

where L is the natural logarithm of D, and x refers to the horizontal position of the draft value along the track. With the further assumption that $L_{x+\Delta/2}$ and $L_{x-\Delta/2}$ are *jointly* normal, the characteristic function of ζ can be straightforwardly determined and from it the pdf. The final result for each ice population is

$$\text{pdf}(\zeta) = \frac{\Delta e^{-m}}{2\pi\sqrt{\sigma_s^2+\sigma_m^2}} \int_{-\infty}^{\infty} e^{-\frac{\{y^2-2\rho' f(y)+f(y)^2\}}{2}} g(y)\,dy \tag{24}$$

where

$$f(y) = \frac{\ln\left(e^{y\sigma'} + \Delta\,|\zeta|\,e^{-m}\right)}{\sigma'}, \tag{25}$$

$$g(y) = \frac{1}{e^{y\sigma'} + \Delta\,|\zeta|\,e^{-m}}, \tag{26}$$

$$\rho' = \frac{\rho\sigma_s^2 + \sigma_m^2}{\sigma_s^2+\sigma_m^2}, \tag{27}$$

and $$\sigma' = \sigma_s \sqrt{1-\rho} \sqrt{\frac{2\sigma_m^2 + (1+\rho)\sigma_s^2}{\sigma_m^2 + \sigma_s^2}} \quad . \tag{28}$$

In the above equations ρ is the correlation between log-draft values separated horizontally by Δ metres.

The draft locations $x + \Delta/2$ and $x - \Delta/2$ are assumed to be in the same pan, i.e. the same segment of that particular ice population. If they are not, the above equations can be modified, in principle, to allow calculations of the cross-pan boundary effects, however, the complexity of the model increases beyond the intentions of this report, with unknown cross-pan ice-population proportions that would need to be specified. For the present purposes, cross-pan effects are generally ignored. The final full pdf(ζ) is the α-weighted sum of the individual pdf's over all ice populations.

Measured pdf's were determined from slopes generated by the FFT process previously described and also by the divided difference process of Eq. (22) with $\Delta = 20$ m, and although the two give very similar results, the latter pdf is the one used here.

When Eqs. (24)-(28) are evaluated using the parameters for each ice population as given in Table 11, and $\Delta = 20$ m, the fit to the measured slope pdf is quite satisfactory, as can be seen in Figure 11. For ice populations 2 to 5 the correlation values ρ are obtained by straightforward

Table 11. Parameters for Computing the Slope Pdf's

Ice population	α	m	σ_m	σ_s
5	0.017	-0.73	0.258	0.35
4	0.0149603	-0.1283	0.0468	0.125
3	0.09612	0.7405	0.068	0.068
2b	0.15689	1.0225	0.113	0.0625
2a	0.25713	1.1696	0.0**	0.238434**
1	0.4631	1.4229	0.0	0.560238

**values in the convolutional model are σ_m=0.230 and σ_s=0.0625

evaluation of the correlation function given in Eq. (8) and Table 3. For population 1 the correlation value is similarly obtained but with a β-parameter that pertains to the entire data set in the linear domain (the A-value is chosen to match the total power to the σ-value of Table 8, i.e. 0.560238, with B and β_0 the same as the entire log spectral values.) Also population 2a is assumed to be a form of background ice, i.e. σ_m for 2a is taken to be zero and σ_s is taken to be

0.238434; without this the fit is much worse than shown. Thus this slope analysis suggests that population 2a may be better identified as background ice. Variations in the value of ρ for ice population 1 alter the level of the tail section in Figure 11b (and also the height of the peak), and cross-pan boundary contributions also affect the tails, mainly producing increased levels. The measured pdf's for steepness greater than 1 become very sporadic for $\Delta = 20$ m because the expected number of counts per bin falls below 1. Table 12 contains the correlation values used in the evaluations of the integral.

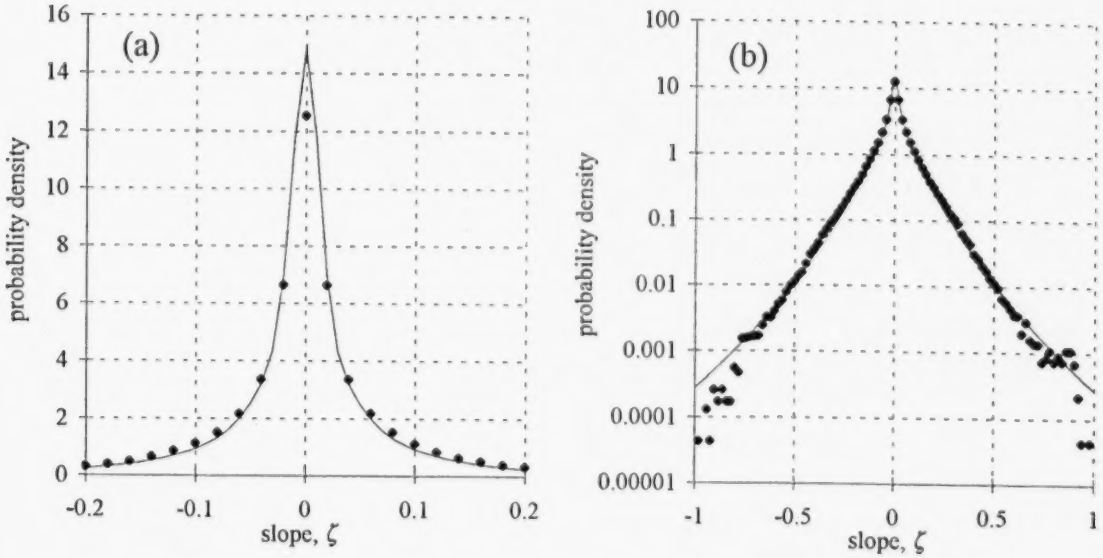

Figure 11. Theoretical and measured slope probability densities. (a) linear scale, (b) logarithmic scale; the symbols (♦) show the data values, and the lines are Eqs. (24)-(28); both use a bin size of 0.02.

Table 12. Correlation Values for Slope Pdf's

Ice population	ρ (20m)	ρ (4m)
5	0.088536	0.198530
4	0.049439	0.110868
3	0.112187	0.281820
2b	0.171887	0.464807
2a	0.650346	0.921217
1	0.653459	0.925627

It is worth noting that the model is not fitted to the data in the figure, instead the model uses parameters estimated from other features of the data—in this case power spectra and draft

pdf's—and so the fit as shown is quite encouraging.

The measured slope pdf as published by Hughes (1991) is also fitted reasonably well by the above integral but with $\Delta = 4$ m.

A simple and effective approximation to the above integral, asymptotically correct as $\Delta|\zeta|\exp(-m) \rightarrow \infty$ for each population, is

$$\text{pdf}(\zeta) = \Delta e^{-m} \frac{e^{-[\ln(1+\Delta\,|\zeta|\,e^{-m})]^2/2\sigma^2}}{\sigma(1+\Delta\,|\zeta|\,e^{-m})\sqrt{2\pi}} \quad . \tag{29}$$

Again, the full pdf(ζ) is the α-weighted sum of these over all ice populations. It can be seen from this equation that large values of $|\zeta|$ are associated with large values of m (otherwise the pdf is vanishingly small). This implies that steep ice occurs most in ice population 1 (and perhaps 2) and that steep ice is found in large draft ice, a conclusion that is further borne out by an examination that has been made of the joint probability density of draft and slope. It can also be seen that the pdf becomes Gaussian as $|\zeta| \rightarrow 0$. Numerical computations bear this out and also show that a completely Gaussian model is strongly deficient in steep slopes.

Ice populations 2b to 5 contribute only to a very narrow range of slopes centered on zero, whereas populations 1 and 2a contribute to the entire range out to ~±1. According to the model, traditional "level" ice ($|\zeta| \leq 0.025$) includes 93% of all population 5 ice and over 97% of populations 4, 3, and 2a ice. Thus it captures virtually all of the ice that is not of population 1 or 2a. The model also shows that 20% and 28% of the level ice field will come from these last two, respectively, but further numerical simulations show that only a few percent (~7.5%) of these are in segments with length > 15 m. The "level" ice criterion (0.025) is thus expected to separate ice populations 1 and 2a from 2b to 5 very well for those longer scales.

7. DISCUSSION AND CONCLUSIONS

It is quite clear from the data that the mean drafts of the pans within each ice population display a range of values, and that the standard deviations also display a range of values. The implication is that the thermodynamic ice-"growing" conditions, including the ages of the individual pans—and perhaps deformations of the ice cover by stress-induced mechanisms—demonstrate a commensurate variability from pan-to-pan. The ranges are not large but they are of some glaciological significance—within ice population 4 the pan means range from 0.8 m to 1.1 m and in ice population 5 from 0.3 m to 0.5 m. The ranges are less significant when interpreted statistically—a sizable proportion of the range of the means, perhaps 40%, can be ascribed to variations inherent in selecting short samples from a single statistical population.

The standard deviations within each ice population are relatively more uniform statistically. Variations of the standard deviations are about the same for the Wadhams and Horne criterion (Eq. (3)) as for the present FFT-based criterion (< ~20%), and the variations are increased somewhat if the criterion is widened. Numerical results show that this level of variation is essentially unimportant in determining the final pdf(D). For modelling purposes it thus seems that a good first approximation is to assume that the standard deviations come from a single underlying value. This leads to the possibility that there is a "generic" kind of ice sheet, one whose roughness is a simple function of its mean thickness, but which is otherwise essentially constant. Its roughness would be due to local-scale variations in conditions and would exhibit some of the features of the (level) ice examined here. The present research would indicate that such a "generic" ice sheet is lognormal, so that its roughness is proportional to its mean draft, and thus its standard deviation in the log domain is constant.

The pan length distributions for lengths of a few metres, as calculated from the data, are likely to be expressions only of single population random sequences rather than indications of features of multiple populations. However, this is apparently not true in general for data pertaining to lengths > 15 m, and certainly not to lengths ~50 m or more. Even so, a firm conclusion concerning whether the relevant pdf's for multiple distribution pans are truly lognormal for each of the distributions, with parameters as given in Table 4, must await further refinements in the analysis or further data (or both). In the meantime, the present results do suggest that the most probable pan length is in the 20-m to 50-m range (and the average pan length is in the 40-m to 100-m range). Because of the heavy weighting of ice population 2a towards lengths of 15 m, as determined from histograms of the means, the question is raised as to whether it is pan ice at all, or whether it is more properly considered as deformed ice but separately distributed from ice population 1. Large draft level ice can exist in very large areas that are essentially autonomous and yet which display peak drafts that are quite different from one another, as has been shown by Melling and Riedel (1996b) in a nearby location. Aside from excessive near-shore ridging that has been observed, perhaps there are other deformed ice regions that are not integrated either.

For numerical simulation of ice sheets based on the *Gurnard* data, perhaps the very simplest approach is not too bad, namely, drawing each ice population from a lognormal statistical population with a *single* mean as well as a single standard deviation. A sizable proportion of the measured variability would automatically be included through random sampling effects. The appropriate parameters would be the α's and σ_m's given in Table 8, and the m's and σ_s's as given there in Table 9 (for this set at least an attempt has been made to remove the effect of the high frequency measurement noise). The present results indicate that a lognormal distribution of lengths with parameters as given here in Table 4, and uncorrelated with the other parameters, would be also appropriate. To go beyond this, the present conclusions indicate that the next level of complexity would be to keep the standard deviations fixed but to allow the means to be normally distributed with parameters as given in Table 7. To go yet further would be to allow for very

small corrections by letting the standard deviations vary according to an Inverse Gauss or gamma distribution with a ratio of the standard deviation to mean in the range of 0.1-0.2.

A complicating (and significant) factor in the examination of spectra and probability density functions of *Gurnard* ice draft is the presence of the high-frequency measurement noise. The standard deviations estimated for population 4 and 5 ice segments in the linear domain have values of 0.1125 m. These must be strongly conditioned by the noise root-mean-square of ~0.1 m, and so estimates of the noise-free values would be considerably less than this (and possibly different for the two ice populations). The log domain values would also be significantly reduced—possibly even to the ~0.05 value obtained for ice populations 2, 3 and 4 by the approximate noise removal method—and thus toward support for the concept of "generic" lognormal ice with a constant σ_s. (The Wiener filter method in this regard does not present nearly such clear results.) The spectra for these pans are also almost completely "masked" by the noise—a situation that is not removed even in the large-draft pans of ice populations 2 and 3. The spectra also show that the fractal nature of the short-scale ice in the pans is totally concealed by the noise for this data set.

It is interesting that the most direct estimates of σ_s that are available from the spectra, namely the square root of the total power calculated from the non-noise spectral portion for ice populations 2, 3 and 4 in the log domain ($\{A^2\pi\beta/4\}^{1/4}$ and Table 3), give values of 0.04 to 0.05, very similar to those obtained by the approximate noise removal method.

The slope distribution is neither Gaussian nor simply lognormal. However it does appear to be predictable from lognormal draft pdf's (after allowing for correlation in the draft-values) and it is lognormal asymptotically for large slopes (positive or negative) for each of the ice populations. Any differences between the model and the measurement pdf's are probably due to the model's omission of pan boundary crossings, and to the difficulty in obtaining accurate estimates for the correlation function of ice population 1. Limiting slopes for the present analysis are ~±1, but this depends strongly on the degree of smoothing that has been applied. The data processing used a smoothing commensurate with Δ~20 m, and it is expected that steeper slopes would exist for less smoothing. (But the smoothing cannot all be removed because the measurement process itself has also imposed some via the finite beamwidth of the sonar.) It appears that steep slopes are preferentially found in large draft ice.

The model indicates that using traditional "level" ice will very effectively separate ice populations 2b to 5 from ice populations 1 and 2a.

8. REFERENCES

Bishop, G. C., and S. E. Chellis 1989. Fractal dimension: a descriptor of ice keel surface roughness, Geophys. Res. Letters, 16 (9).

Hughes, B. A. 1991. On the use of lognormal statistics to simulate one- and two-dimensional under-ice draft profiles, J. Geophys. Res., 96, 22101-22111.

Key, J., and A. S. McLaren 1991. Fractal nature of the sea ice draft profile, Geophys. Res. Letters, 18 (8), 1437-1440.

McLaren, A. S. 1989. The under-ice thickness distribution of the Arctic Basin as recorded in 1958 and 1970, J. Geophys. Res., 94, 4971-4983.

Melling, H., and D. A. Riedel 1995. The underside topography of sea ice over the continental shelf of the Beaufort Sea in the winter of 1990. J. Geophys. Res., 100(C7), 13641-13653.

Melling, H., and D. A. Riedel 1996a. The development of seasonal ice in the Beaufort Sea during the winter of 1991-92: A view from below. J. Geophys. Res., 101(C5), 11975-11991.

Melling, H., and D. A. Riedel 1996b. The thickness and ridging of pack-ice causing difficult shipping conditions in the Beaufort Sea, Summer 1991. Atmosphere-Ocean, 34, 457-487.

Press, W. H., S. A. Teukolsky, W. T. Vetterling, and B. P. Flannery 1992. Numerical Recipes in C, 2nd ed., Cambridge University Press, New York.

Wadhams, P. 1981. Sea-ice topography of the Arctic Ocean in the region of 70°W to 25°E, Philos. Trans. R. Soc. London, Ser. A, 302, 45-85.

Wadhams, P., and R. J. Horne 1980. An analysis of ice profiles obtained by submarine in the Beaufort Sea, J. Glaciol., 25, 401-424.

APPENDIX

Standard Deviation Variability Test Analysis

The test being considered is for variability in estimates of standard deviation (or variance) of different length samples drawn from correlated Gaussian data. The analysis is quite straightforward—define a statistic s in terms of an average of the relevant function of $\ln(D)$, compute the mean and variance of this statistic, and compare the scatter in the data to this variance. Because the analysis is limited to those pans which are longer than 15 m, there are always 15 data points or more (often hundreds) in the averages, therefore it is appropriate to invoke the Central Limit Theorem (i.e. Gaussian formulae) to calculate the 95% values from this computed mean and variance (and then determine whether 95% of the measured data fall within these values). As an intermediate step the effective number of independent points, l, in the averaging length, n, is determined. The analysis follows, and it is given in detail for the variability of a statistic M defined to approximate the mean μ, because its formulae are more straightforward than those pertaining to the standard deviation statistic s. In the following, both μ and σ are taken to be δ-like, with locations of m and σ_S respectively. With $\xi_i = \ln(D_i)$, where i is the horizontal position number of the sample within the pan,

$$M = \frac{1}{n}\sum_{i=1}^{n}\xi_i \ , \tag{A1}$$

$$m_M \equiv \langle M \rangle = \langle \xi_i \rangle = m \quad \text{(independent of } i\text{)}, \tag{A2}$$

$$\begin{aligned}\sigma_M^2 &\equiv \langle M^2 \rangle - \langle M \rangle^2 \\ &= \frac{1}{n^2}\sum_{i=1}^{n}\sum_{j=1}^{n}\langle \xi_i \xi_j \rangle - m^2\end{aligned} \tag{A3}$$

The ξ-process (i.e. the draft data sequence) is considered to be locally stationary so that the covariance is a function only of the separation, not of the location itself. Thus $\langle \xi_i \xi_j \rangle$ is a function only of i-j, and because of the symmetry in its definition it is a function only of $|i\text{-}j|$. The m^2-factor can be included in the angle-bracket term—shifting each ξ by m—and the normalized version of the result (the correlation function) designated as C_k, where $k=i\text{-}j$, and $C_k = \langle (\xi_i - m)(\xi_j - m) \rangle / \sigma^2{}_s$.

Because of the stationarity the double sum in Eq. (A3) can be converted into a single weighted sum over twice the range. The final result is

$$\begin{aligned}\sigma_M^2 &= \frac{\sigma_s^2}{n^2}\sum_{k=-n+1}^{n-1}(n-|k|)C_k \\ &= \sigma_s^2\{\frac{1}{n}+\frac{2}{n^2}\sum_{k=1}^{n}(n-k)C_k\} \\ &= \sigma_s^2\{\frac{1}{n}+\frac{2S_n}{n}-\frac{2T_n}{n^2}\} \equiv \frac{\sigma_s^2}{l_M(n)}\end{aligned} \tag{A4}$$

Here S_n and T_n are $\sum C_k$ and $\sum kC_k$ respectively, each summed from 1 to n. A similar analysis can be performed on s, defined as

$$s^2 = \frac{1}{n}\sum_{i=1}^{n}(\xi_i - M)^2 \tag{A5}$$

with 4th-order moments of ξ appearing for the variance of s^2 (which are reducible to 2nd-order moments because of the Gaussian character of ξ), and a correspondingly more complicated form for the dependence of var(s^2) on n. Using forms that are analogous to those for uncorrelated ξ's, the following formulae can be usefully defined:

$$\begin{aligned}\langle s^2\rangle &= \sigma_\xi^2\frac{l_1-1}{l_1}\ , \\ \mathrm{var}(s^2) &= 2\sigma_\xi^4\frac{l_2-1}{l_2^2}\ , \\ \mathrm{var}(s^2) &= \frac{\sigma_\xi^4}{l_3}\ .\end{aligned} \tag{A6}$$

Here l_1, l_2, and l_3 are measures of the number of independent points in the sample. They are all functions of n, analogous to l_M above, and are all straightforwardly determinable. l_1 is in fact identical to l_M, and is given explicitly below, but l_2 and l_3 are algebraically quite complicated and are not reproduced here. The formula in Eq. (A6) defining l_2 is appropriate if s^2 has a χ^2 distribution, with l_2 as the number of independent points, and the formula defining l_3 is appropriate if s^2 has a Gaussian distribution (from these two formulae it is apparent that l_3 is quite simply related to l_2). Explicitly,

$$l_1 = l_M = \frac{n}{1+2S_n-\frac{2T_n}{n}}\ . \tag{A7}$$

By appealing to the Central Limit Theorem, s^2 is taken to be Gaussian (for large enough n) and the 95% confidence limits are seen to be at

$$s^2_{95\%} = \sigma_s^2 \left\{ \frac{I_1 - 1}{I_1} \pm \frac{1.96}{\sqrt{I_3}} \right\}$$

$$= \langle s^2 \rangle \left\{ 1 \pm \frac{1.96 I_1}{(I_1 - 1)\sqrt{I_3}} \right\} \qquad \text{(A8)}$$

where, to evaluate this last equation, $\langle s^2 \rangle$ is replaced by its estimate from the data. (To fit the data better this estimate is made as a function of n and is given the form $a + b/\sqrt{n}$.) With this definition, 95% of the samples should be between the value calculated with the + sign and the value calculated with the - sign. A similar equation can be obtained for $M_{95\%}$. Using computer-generated Gaussian deviates, filtered to display the same correlation as the measured data, these equations have tested and have been shown to be valid.

I_1, I_2, and I_3 were computed using the correlation functions obtained from the spectra (Eq. (8) for each ice type), and the confidence lines as functions of n computed from the above formulae.